Communication

# Study of Quasi-Monodisperse InO Nanocrystals: Synthesis and Optical Determination

Qingsheng Liu, Weigang Lu, Aihui Ma, Jinke Tang, Jun Lin, and Jiye Fang

*J. Am. Chem. Soc.*, **2005**, 127 (15), 5276-5277• DOI: 10.1021/ja042550t • Publication Date (Web): 23 March 2005



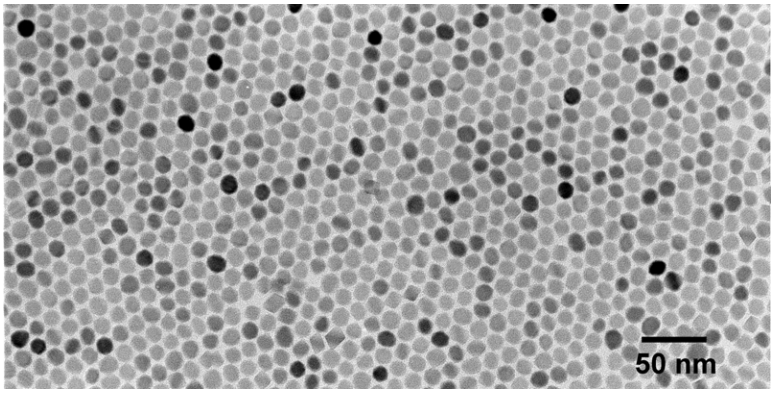


## More About This Article

Additional resources and features associated with this article are available within the HTML version:

- Supporting Information
- Links to the 21 articles that cite this article, as of the time of this article download
- Access to high resolution figures
- Links to articles and content related to this article
- Copyright permission to reproduce figures and/or text from this article

View the Full Text HTML

J|A|C|S
COMMUNICATIONS

Published on Web 03/23/2005

# Study of Quasi-Monodisperse $In_2O_3$ Nanocrystals: Synthesis and Optical Determination

Qingsheng Liu,[†,‡] Weigang Lu,[†,‡] Aihui Ma,[‡] Jinke Tang,[§] Jun Lin,[¶] and Jiye Fang*[,†,‡]

*Department of Chemistry, AMRI, and Department of Physics, University of New Orleans, New Orleans, Louisiana 70148, and Key Lab of Rare Earth Chemistry and Physics, Changchun Institute of Applied Chemistry, Chinese Academy of Sciences, Changchun 130022, P. R. China*

Received December 11, 2004; E-mail: jfang1@uno.edu

Indium oxide ($In_2O_3$) has been used widely for ultra-sensitive toxic gas (such as $NO_2$[1] and $NH_3$[2]) detectors, transparent conductors,[3] solar cells, and optoelectronic devices.[4] It is anticipated that low-dimensional $In_2O_3$ may exhibit some unique properties, including novel optical behaviors.[5,6] Although various types of $In_2O_3$, including 2D (i.e., thin films)[7,8] and 1D (i.e., nanowires)[9−11] structures, have been extensively prepared and investigated, few reports were concentrated on $In_2O_3$ quantum dots (0D).[12,13] Synthesis and study of high-quality and monodisperse $In_2O_3$ nanocrystals (NCs) as 0D quantum-confined materials are still essential and significant. In this communication, we report our synthesis of single-crystal, quasi-monodisperse $In_2O_3$ NCs, as well as the optical observation from these NCs.

All of the chemicals were used as received from Aldrich without further purification. In a typical experiment, 0.40 mmol of indium acetate (99.99%), 0.55 mL of oleylamine (70%), and 0.60 mL of oleic acid (90%) were combined with 7.0 mL of hexadecane (>99%) in a three-neck flask equipped with a condenser. The system was vacuumed at room temperature and at 110 °C for a while, respectively, to form a clear light-green solution. At 110 °C, 1.45 mmol of trimethylamine *N*-oxide (TMNO, 98%) was subsequently introduced into this vigorously stirred hot mixture under an argon stream. The temperature of this system was then increased to 120 °C, where it remained for 1 h under agitation and argon protection. The color of the solution gradually turned light-yellow. The temperature was further increased to 290 °C at a rate of 10 °C/min for an additional 35 min reflux. The mixture was clear-brown during the first 5 min at 290 °C, and subsequently changed to a yellow turbid slurry during the following 25 min, and finally turned clear again. These colloids were cooled to room temperature by quickly removing the heating source, and then isolated by adding a sufficient amount of ethanol and separating with centrifugation. The yielded precipitate was redispersed in hexane followed by centrifugation to remove the very small amount of insoluble aggregates. The morphology and phase structure were evaluated using a transmission electron microscope (TEM) (JEOL 2010) and an X-ray diffractometer (XRD) (Philips X-pert system), respectively. We realized that the ratio of oleic acid and oleylamine was a key factor to form $In_2O_3$ NCs. Oleic acid without oleylamine and TMNO would not result in any NCs; if TMNO with oleic acid were introduced into the reaction without oleylamine, only indium hydroxide would form according to the results of our XRD analyses; whereas a high content of oleylamine without oleic acid and TMNO would make the NCs rapidly grow and aggregate. We also realized that the TMNO acts as not only a sole oxidizing agent. In addition, it was determined that the reaction temperature is another important parameter which affects the morphology and size of $In_2O_3$ NCs. The lower the reaction temperature, the smaller the NCs produced. Moreover, these small NCs generally associate with irregular shape and broad size distribution. A typical TEM image in low magnification is shown in Figure 1a, exhibiting quasi-monodisperse and hexagonally packed $In_2O_3$ NCs with an average diameter of 11.5 nm. It can be further seen that a short-range, hexagonal order of $In_2O_3$ NCs can be self-assembled in an area as large as a few square micrometers (Figure S1 in the Supporting Information). The high-resolution TEM image in Figure 1b reveals the fringes from the continuous lattice structure of a typical crystallite, indicating that these $In_2O_3$ NCs possess high crystallinity.

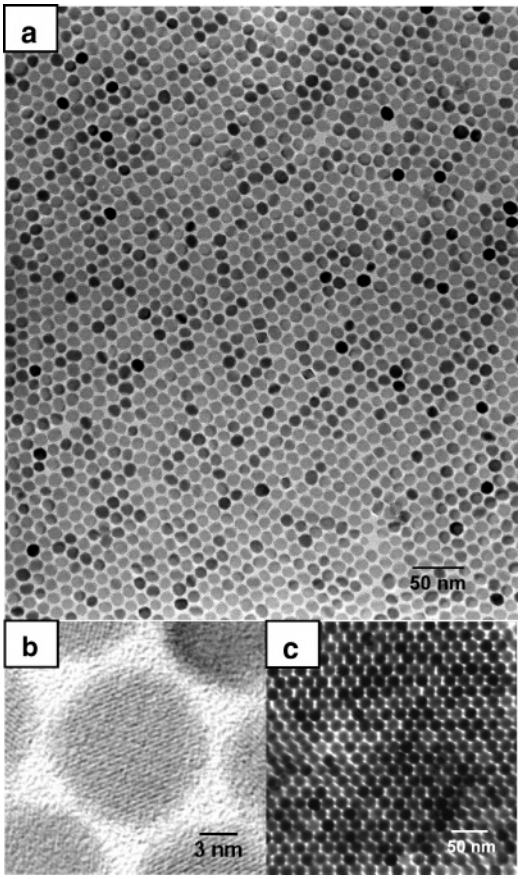


***Figure 1.*** (a) Bright field TEM image of 11.5 nm $In_2O_3$ NCs (monolayer assembly); (b) HRTEM of a single 13.5 nm $In_2O_3$ NC; (c) TEM image of a 3D superlattice of 20.0 nm $In_2O_3$ NCs.

It is generally believed that for a primarily formed single-phase crystal with ultra-small size, the surface must be a polyhedron containing high-index crystallography planes[14] which have a tendency to grow along direction(s) where the facet(s) possess low

[†] Department of Chemistry.
[‡] AMRI.
[§] Department of Physics.
[¶] Changchun Institute of Applied Chemistry.



**10.1021/ja042550t CCC: $30.25** 

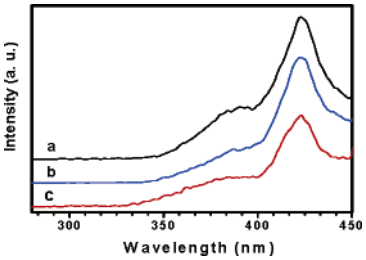


***Figure 2.*** Photoluminescence spectra of $In_2O_3$ in various sizes: (a) 20.0 nm; (b) 13.5 nm; and (c) 11.5 nm.

surface energy. To provide enough primary clusters for keeping a constant rate of the crystal growth to produce larger NCs, we adopted a dynamic injection technique,[15,16] which has been employed previously and is favorable for continuous growth of NCs. For instance, a portion of the above-mentioned reaction mixture being heated at 120 °C for 1 h (referred to as "precursor") could be stored at room temperature, reinjected into the same mixture after a reflux at 290 °C for 40 min, and maintained at the same temperature for an additional 30 min. Such processing would tune the average size of $In_2O_3$ NCs from 11.5 to 13.5 nm in diameter (Figure S2). Application of multiple injections using the same technique achieved the average size of $In_2O_3$ NCs up to ∼20 nm. One of the 3D superlattice TEM images of 20.0 nm NCs assembled by slowly evaporating the alcohol-containing[14] solvent is presented in Figure 1c. To explore the size distribution, three $In_2O_3$ samples dispersed in hexane were determined using dynamic light scattering technique (Protein Solution DynaPro 99 Molecular Sizing Instrument). Figure S3a−c illustrates the size histogram of three $In_2O_3$ samples, indicating highly narrow distributions of these colloids. The light scattering results further reveal that the mean hydrodynamic radii of three samples are 7.3, 8.9, and 12.6 nm, which considerably coincide with the diameters measured from the TEM images, that is, 11.5, 13.5, and 20.0 nm, respectively, as the thickness of the capped organic layer is estimated at ∼2 nm.

Figure S4 presents the XRD patterns of three samples with different sizes, indicating a cubic phase from these NCs because all of the detectable diffraction peaks are indexed to those from body-center cubic $In_2O_3$ (ICDD PDF card No. 06-0416). The average sizes of crystallites estimated from XRD patterns by applying the Scherrer equation[17] are close to those calculated from TEM images. For example, the average size estimated from the pattern "a" in Figure S4 is ∼10.5 nm, which is well close to that determined from TEM image of this sample (11.5 nm). This good agreement confirms the TEM observation; that is, each individual $In_2O_3$ particle is a single crystal.

Cubic $In_2O_3$ is an n-type semiconductor due to its oxygen-deficient fluorite structure with twice the unit-cell edge of the corresponding fluorite cell and with $^1/_4$ of the anions missing in an ordered way.[7,8,18] Furthermore, different processing routes may lead to varied oxygen vacancies. The oxygen vacancies can act as donors and would induce the formation of new energy levels in the band gap, which results in photoluminescence (PL) under photoexcitation process. Though the PL emission mechanism of $In_2O_3$ is still ambiguous, it is believed that the blue PL peaks found in previous work[9,19] are mainly attributed to deeper energy level emissions. It is well-known that bulk $In_2O_3$ cannot emit UV emission at room temperature. Nevertheless, a UV emission peak has been reported by Cao et al.,[10] who attributed the appearance of UV emission to high crystal quality of $In_2O_3$. In Figure 2, a relatively strong PL peak centered at 423 nm and a shoulder located at about 392 nm in all of the studied samples can be clearly seen when they were excited at 234 nm at room temperature (Figure S5, PL were carried out on a Perkin-Elmer LS 55 luminescence spectrometer). In our samples, no additional emission peak was observed, and the results from TEM and XRD do support Cao's explanation. On the other hand, the maximum absorption peaks of $In_2O_3$ synthesized via this method show up at ∼305 nm (Figure S6), which exhibits a certain phenomena of blue shift in comparison with the bulk $In_2O_3$ (about 330 nm).[20,21] In addition, previous reports[13,22] indicate that weak quantum-confinement-effects may still be detected even if the size of $In_2O_3$ NCs is slightly larger than the Bohr radius. On the basis of these results, it is suggested that the appearance of UV emission from the $In_2O_3$ NCs synthesized in this work is partially due to weak quantum-confinement-effects.

In summary, we have successfully synthesized quasi-monodisperse $In_2O_3$ NCs with high crystallinity in a high-temperature organic solution. The average size of NCs can be tuned using a dynamic injection technique. TEM and XRD investigations indicate that each NC is a single crystal. The optical determination implies that the PL behavior of these $In_2O_3$ NCs is different from that of the bulk, probably due to the combination of weak quantum-confinement-effects and the nature of high crystallinity in NCs.

**Acknowledgment.** This work was supported by NSF CAREER program (DMR-0449580), BSST LCC, and AMRI. Professors Fang and Lin are very grateful for the financial support by the two-base program (00310530) and NSFC programs (50225205, 20431030). We also thank Poncho De Leon for his help in polishing the context.

**Supporting Information Available:** Figures S1−S6. This material is available free of charge via the Internet at http://pubs.acs.org.

## References

(1) Zhang, D.; Liu, Z.; Li, C.; Tang, T.; Liu, X.; Han, S.; Lei, B.; Zhou, C. *Nano Lett.* **2004**, *4*, 1919−1924.
(2) Zhang, D.; Li, C.; Liu, X.; Han, S.; Tang, T.; Zhou, C. *Appl. Phys. Lett.* **2003**, *83*, 1845−1847.
(3) Gordon, R. G. *MRS Bull.* **2000**, *25*, 52−57.
(4) Gopchandran, K. G.; Joseph, B.; Abraham, J. T.; Koshy, P.; Vaidyan, V. K. *Vacuum* **1997**, *48*, 547−550.
(5) Kityk, I. V.; Ebothé, J.; Hichou, A. E.; Idrissi, B. E.; Addou, M.; Krasowski, J. *J. Opt. A: Pure Appl. Opt.* **2003**, *5*, 61−65.
(6) Ederth, J.; Hultåker, A.; Heszler, P.; Niklasson, G. A.; Granqvist, C. G.; Doorn, A. v.; Haag, C. v.; Jongerius, M. J.; Burgard, D. *Smart Mater. Struct.* **2002**, *11*, 675−678.
(7) Tamaki, J.; Naruo, C.; Yamamoto, Y.; Matsuoka, M. *Sens. Actuators, B* **2002**, *83*, 190−194.
(8) Liess, M. *Thin Solid Films* **2002**, *410*, 183−187.
(9) Liang, C.; Meng, G.; Lei, Y.; Phillipp, F.; Zhang, L. *Adv. Mater.* **2001**, *13*, 1330−1333.
(10) Cao, H.; Qiu, X.; Liang, Y.; Zhu, Q.; Zhao, M. *Appl. Phys. Lett.* **2003**, *83*, 761−763.
(11) Kam, K. C.; Deepak, F. L.; Cheetham, A. K.; Rao, C. N. R. *Chem. Phys. Lett.* **2004**, *397*, 329−334.
(12) Murali, A.; Barve, A.; Leppert, V. J.; Risbud, S. H.; Kennedy, I. M.; Lee, H. W. H. *Nano Lett.* **2001**, *1*, 287−289.
(13) Seo, W. S.; Jo, H. H.; Lee, K.; Park, J. T. *Adv. Mater.* **2003**, *15*, 795−797.
(14) Murray, C. B.; Kagan, C. R.; Bawendi, M. G. *Annu. Rev. Mater. Sci.* **2000**, *30*, 545−610.
(15) Qian, C.; Kim, F.; Ma, L.; Tsui, F.; Yang, P.; Liu, J. *J. Am. Chem. Soc.* **2004**, *126*, 1195−1198.
(16) Lu, W.; Gao, P.; Jian, W. B.; Wang, Z. L.; Fang, J. *J. Am. Chem. Soc.* **2004**, *126*, 14816−14821.
(17) Cullity, B. D. *Elements of X-ray Diffraction*, 2nd ed.; Addison-Wesley: Reading, MA, 1978.
(18) Williams, D. E. *Sens. Actuators B* **1999**, *57*, 1−16.
(19) Zhou, H.; Cai, W.; Zhang, L. *Appl. Phys. Lett.* **1999**, *75*, 495−497.
(20) Wen, S. J.; Campet, G.; Portier, J.; Couturier, G.; Goodenough, J. B. *Mater. Sci. Eng. B* **1992**, *14*, 115−119.
(21) Hamberg, I.; Granqvist, C. G. *Sol. Energy Mater.* **1986**, *14*, 241−256.
(22) Yu, D.; Wang, D.; Qian, Y. *J. Solid State Chem.* **2004**, *177*, 1230−1234.

JA042550T